

Volume 6, No. 3; June 2018

Advances in Image And Video Processing

ISSN: 2054-7412

TABLE OF CONTENTS

EDITORIAL ADVISORY BOARD	I
DISCLAIMER	II
Statistical Evaluation of The Heavy Metals in the Sediments of Warri River and Environs P. N. Jire, E.G. Imeokparia	1
Traffic Sign Detection and Recognition for Driving Assistance System Huei-Yung Lina, Chin-Chen Chang, Shu-Chun Huang	17
A Logic Circuit Simulation for Finding Identical or Redundant Files using Counter and Register Lianly Rompis	26

EDITORIAL ADVISORY BOARD

Editor in Chief

Dr Zezhi Chen

Faculty of Science, Engineering and Computing
Kingston University London
United Kingdom

Professor Don Liu

College of Engineering and Science, Louisiana Tech
University, Ruston,
United States

Dr Lei Cao

Department of Electrical Engineering, University of
Mississippi,
United States

Professor Simon X. Yang

Advanced Robotics & Intelligent Systems (ARIS)
Laboratory, University of Guelph
Canada

Dr Luis Rodolfo Garcia

College of Science and Engineering, Texas A&M
University, Corpus Christi
United States

Dr Kyriakos G Vamvoudakis

Dept of Electrical and Computer Engineering, University
of California Santa Barbara
United States

Professor Nicoladie Tam

University of North Texas, Denton, Texas
United States

Professor Shahram Latifi

Dept. of Electrical & Computer Engineering University of
Nevada, Las Vegas
United States

Professor Hong Zhou

Department of Applied Mathematics Naval Postgraduate
School Monterey, CA
United States

Dr Yuriy Polyakov

Computer Science Department, New Jersey Institute of
Technology, Newark
United States

Dr Rodney Weber

School of Mathematics and Statistics
University College, Australian Defence Force Academy,
Australia

Dr Cornelia Laule

Dept. of Pathology and Laboratory Medicine
The University of British Columbia
Canada

Dr Yiqiang Q. Zhao

School of Mathematics and Statistics
Carleton University, Ottawa, Ontario
Canada

Dr Farouk YALAOUI

LOSI(Optimization Laboratory of Industrial Systems)
University of Technology of Troyes
France

Dr Daniel Berrar

School of Biomedical sciences
Ulster University
United Kingdom

Dr Ozlem Uzuner

Department of Information Studies
State university of New York
United States

Dr Erik L. Ritman

Psychology and Biomedical Engineering, Mayo Clinic,
State of Minnesota
United States

Dr Pascal Hitzler

Dept. of Computer Science and Engineering
Wright State University
United States

Dr Thomas D. Parsons

Dept. of Psychology
University of North Texas
United States

Dr Eric Hoffman

Department of Radiology
University of Iowa,
United States

Dr Salil Kanhere

Department of Computer Science and Engineering
University of New South Wales
Australia

Dr Maolin Tang

Department of Electrical Engineering and Computer
Science, Queensland University of Technology
Australia

Dr Simon X. Yang

Department of Engineering
University of Guelph
Canada

Dr Francisco Sepulveda

Department of Computer Science
University of Essex
United Kingdom

Dr Yutaka Maeda

Department of Electrical and Electronics Engineering
Kansai University
Japan

Dr Chin-Diew Lai

Department of Statistics
Massey University
New Zealand

Dr Ibrahim Ozkan

Department of Economics
Hacettepe University, Turkey

Dr Henry Schellhorn

Institute of Mathematics Sciences
Claremont Graduate University,
United States

Dr Laurence Devillers
Informatics Laboratory for Mechanics and Engineering
Sciences, University of Paris
France

Dr Stefan Kopp
Social Cognitive Systems Group, Bielefeld University
Germany

Dr A. K. Louis
Institute for Numerical and Applied Mathematics,
Saarland University
Germany

Dr Barry O'Sullivan
University College Cork (UCC)
Ireland

Dr Sabato Manfredi
University of Naples Federico
Italy

Dr Sergio Baragetti
Machine Design and Computational Mechanics
University of Bergamo, Italy

Dr Itamar Ronen
Department of Radiology
Leiden University Medical Centre
Netherlands

Dr Elli Androulaki
Zurich Research Laboratory, Zurich
Switzerland

Dr Jonathan Vincent
Department of IT
Bournemouth University
United Kingdom

Dr Gerard McKee
School of Systems Engineering
University of Reading
United Kingdom

Dr Jun Hong
Department of Computer Science
Queen's University Belfast
United Kingdom

Dr. Ig-Jae Kim
Imaging Media Research Center, Korea Institute of
Science and Technology, Seoul
South Korea

Dr. Reinhard Klette
School of Engineering, Computer and Mathematical
Sciences, Auckland University of Technology
New Zealand

Dr. Constantine Kotropoulos
Department of Informatics, Aristotle University of
Thessaloniki
Greece

Dr. Jun Ohta
Graduate School of Materials Science, Nara Institute of
Science and Technology (NAIST)
Japan

Prof. Klaus Hanke
Surveying and Geoinformation Unit
University of Innsbruck
Austria

Dr Jeff Schneider
School of Computer Science
Carnegie Mellon University,
United States

Dr Alexander J. Smola
Machine Learning Department
Carnegie Mellon University
United States

Dr Debmalya Panigrahi
Department Computer Science
Dule University
United States

Dr Chuck Jacobs
Machine Learning Group, Microsoft
United States

Dr Geoffrey Zweig
Natural Language Processing Group
JP Morgan
United States

Dr Gang Wang
Department of Computer Science
University of California, Santa Barbara
United States

Dr Christino Tamon
Department of Computer Science
Clarkson University
United States

Dr Paul S. Rosenbloom
Department of Computer Science
University of Southern California
United States

Dr Babak Forouraghi
Department of Computer Science
Saint Joseph's University
United States

Dr Haibo He
Department of Electrical, Computer, and Biomedical
Engineering, University of Rhode Island
United States

Dr. Ibrahim Abdulhalim
Department of Electro-Optics Engineering,
Ilse Katz Institute for Nanoscale Science and
Technology, Ben Gurion University
Israel

Prof. Dr. Erik Cuevas
Department of Electronics, Universidad de Guadalajara
Mexico

Prof. Dr. Bernard De Baets
KERMIT, Dept. of Mathematical Modelling Statistics and
Bioinformatics, Ghent University
Belgium

Dr. Joachim Denzler
Computer Vision Group, Institute for Informatics
Friedrich-Schiller-University Jena
Germany

Dr. Antonio Fernández-Caballero
Universidad de Castilla-La Mancha
Spain

DISCLAIMER

All the contributions are published in good faith and intentions to promote and encourage research activities around the globe. The contributions are property of their respective authors/owners and the journal is not responsible for any content that hurts someone's views or feelings etc.

Statistical Evaluation of The Heavy Metals in the Sediments of Warri River and Environs

P. N. Jire ¹, E.G. Imeokparia ²

^{1,2}*Department of Geology, University of Benin, Benin City, Nigeria*
g_imeokparia@yahoo.com

ABSTRACT

This study was carried out to assess and characterize the pollution/contamination status of the sediments in Warri River and its environs in view of the increasing level of oil spillages induced by willful acts of vandalization, lack of maintenance of pipelines, aging facilities, accident, illegal bunkering, petroleum refinery and production, urbanization, industrial activities and indiscriminate dumping of wastes.

A total of thirty-two sediments samples were collected from eight sampling stations, grouped into locations B1-B8 respectively and analyzed for heavy metals. The chemical data set generated were subjected to principal component analysis (PCA)/factor analysis (FA) and Hierarchical cluster analysis (HCA) to determine the subtle factors responsible for their distribution. The heavy metal concentrations of locations B1-B8 were further evaluated using enrichment factor (EF), Contamination factor (CF) and Pollution load index (PLI) to assess the level of pollution in the area.

The Factor Analysis results revealed four sources of pollutants which are explained by four factors (1)petroleum production, oil spills and illegal bunkering/pipe line vandalization (2) iron/steel industries (3)vehicular emission(4) indiscriminate dumping of waste. The R and Q mode cluster analysis yielded three clusters respectively. The Contamination Factor (CF)showed that the sediments have considerable level of Cr contamination at locations B2, B3,B4 and B6 while Fe, Zn, Ni, V, Pb, Cd, Mn and Cu exhibited moderate contamination at locations B1-B7.The Pollution Load Index (PLI)revealed that locations B1-B6 shown progressive site deterioration with respect to the nine measured heavy metals. The Enrichment Factor (EF) indicated that Cr was moderately enriched at locations B1, B2, B4 and B6 while Zn, Ni, Cu, Cd, Mn, Fe, V, and Pb in the sediments ranged from background concentration to minimal enrichment.

Since these heavy metals can become a threat to vegetation and animals and ultimately to humans through the food chain, it is important to continuously monitor the level of pollutants in the environment.

1 Introduction

In the last century a growing and rapidly industrializing world has produced greater quantities of common pollutants such as household garbage, sewage and more toxic and persistent contaminants like pesticides, polychlorinated biphenyls (PCBs), dioxin, chlorofluorocarbons (CFCs), heavy metals, radioactive waste, releases from manufacturing and petroleum exploration and production installations and others.

According to Ndiokwere (2004) pollutants affect the ecosystems in a variety of ways. Pesticides and heavy metals may harm exposed organisms by being acutely toxic or by accumulating in plant and animal tissues through repeated exposures.

Trace amounts of heavy metals are always present in fresh waters from terrigenous sources such as weathering of rocks resulting into geochemical recycling of heavy metal elements in these ecosystems (Blaser et al; 2000, Sekabira et al, 2010).

Volcanoes have been reported to emit high levels of Al, Zn, Mn, Pb, Ni, Cu and Hg along with toxic and harmful gases (Seaward and Richardson 1990). Wind dust which arises from desert region such as Sahara, has high levels of Fe and lesser amounts of Mn, Zn, Cr, Ni and Pb (Ross, 1994). The contribution to ecosystem of elements from sea sprays and mist, often transported many kilometres in land is widely recognized. Cu and Mn from such marine sources have been detected in rain water input to terrestrial environments.(Vermette and Bingham, 1986. In addition heavy metals may enter into aquatic ecosystems from anthropogenic sources such as industrial waste water discharges sewage wastewater, fossil fuel combustion and atmospheric deposition (Ross 1994, Linnik and Zubenko, 2000, Lwanga et al 2003, Idress, 2009).

Contamination of surface and subsurface environment by heavy metals has established the need to understand metal soil/sediment interactions. Trace elements may be immobilized within the stream sediments and thus could be involved in absorption, co-precipitation and complex formation (Salomons and Forstnes, 1980, Mohiuddin et al 2010).

Warri is a medium sized metropolitan city in the Niger Delta area of Southern Nigeria. It is characterized by extensive petroleum exploration, production and petrochemical activities. It's urbanization has also been dominated by timber and sawmill industries, discharge of untreated sewage into the river systems and generation of municipal wastes containing among others spent motor oils from numerous roadside mechanic workshops (Imeokparia et al., 2009).

This study aims at assessing the geochemistry of the stream sediments of warri river and its tributaries so as to establish the possibility of secondary pollution and determine the source apportionment of heavy metals, using statistical and environmental parameters.

2 The Study Area

Warri is among the fastest growing cities in Southern Nigeria. The city is located within the tropical rainforest belt dominated by abundant rainfall (Egborge 2001).The annual ten-year mean is about 2652mm while the mean daily temperature is 31.20C (Nigerian Meteorological Agency, 2003).

The Warri River is among the four major coastal rivers of Delta State, Nigeria, and ranks as one of the most commercially utilized rivers in the Niger Delta of Nigeria. It stretches within Latitudes $5^{\circ} 21' - 6^{\circ} 00' N$ and Longitude $5^{\circ} 24' - 6^{\circ} 21' E$ and covers a surface area of 255sq.km with length of about 150km (NEDECO, 1954). It flows from its source around UtagbaUno in a South-west direction through Ovirie and Ovu inland; and southwards at Odiete through Agbarho to Otokutu. Thereafter it turns south west to Effurun and Warri. Important land marks in this river stretches are Enerhen, Igbudu, Ovwian and the industrial towns of Aladja and Warri. (NEDECO, 1954). Three important creeks empty their waters into the main channel of the river. The first is the Miller Creek which drains the densely populated area of Okere in Warri while the other creeks are Tori and Crawford.

The Warri River is joined by series of tributaries on which are located some Itsekiri villages such as Ode-Itsekiri, Orugbo and an Ijaw village – Ogbeljaw in the south-east direction (Egborge, 1991). The

river drains these tributaries and empties into the brackish Forcados River which in turn empties into the Atlantic Ocean (Benka-Coker, 1983). According to NEDECO (1954), the Warri River and its tributaries are influenced by oceanic tidal variations from Warri to Forcados (Nigerian Navy, 1982).

3 Geology

The study area is underlain by the deposits of the Quaternary Sombreiro-Warri Deltaic Plain Sands that conformably overlie the Benin Formation (Wigwe, 1975) (Fig.1). This Formation consists of fine to medium and coarse-grained unconsolidated sands that are often feldspathic, with 30 - 40 wt% feldspars and occasionally gravelly. This sequence is locally stratified with peat and lenses of soft and plastic clay that could be sandy. The Formation generally does not exceed 120 metres in thickness and it is predominantly unconfined.

Unfortunately, this near surface and shallow Quaternary cover appears not to have received as much attention. The practice has been to generally lump these deposits of alternating fine-medium-grained sands, silts and subordinate lensoid clays together as the recent and present day deposition of sediments on the Benin Formation (Amajor, 1991). However, these important deposits possess distinct characteristics and engineering properties (Bam, 2007), and cover more than 70 per cent of the land surface of Delta State, Nigeria. They are exploited for glass sands and quarried extensively for building purposes (Bam, 2007; Akpokodje and Etu-Efeotor, 1987; Ministry of Commerce and Industry, 2001; Atakpo and Akpoborie, 2011). Furthermore, they constitute the shallow aquifers that are exploited by shallow (<30m) boreholes and dug wells that serve as the primary water supply source for rural as well as many sub-urban and urban communities.

The quality of water yielded is also very crucial but various studies (Ejechi et al., 2007; Akpoborie et al. 2000; Olobaniyi et al. 2007; Abimbola et al. 2002) have indicated that these shallow aquifers are highly vulnerable to contamination from surface sources resulting in quality being compromised.

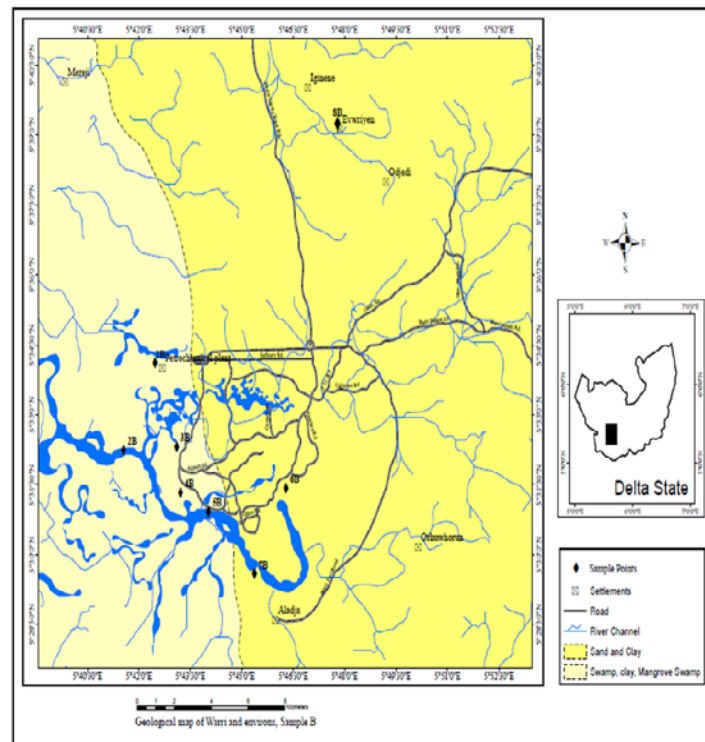


Figure. 1: Geology of Warri and Environs, showing also sample location

4 Materials and Methods

Stream sediments were collected along the Warri River, its three principal creeks and control points at Ewriyen during the raining and dry season (Figs. 2 and 3). GPS was used for the location of sample points.

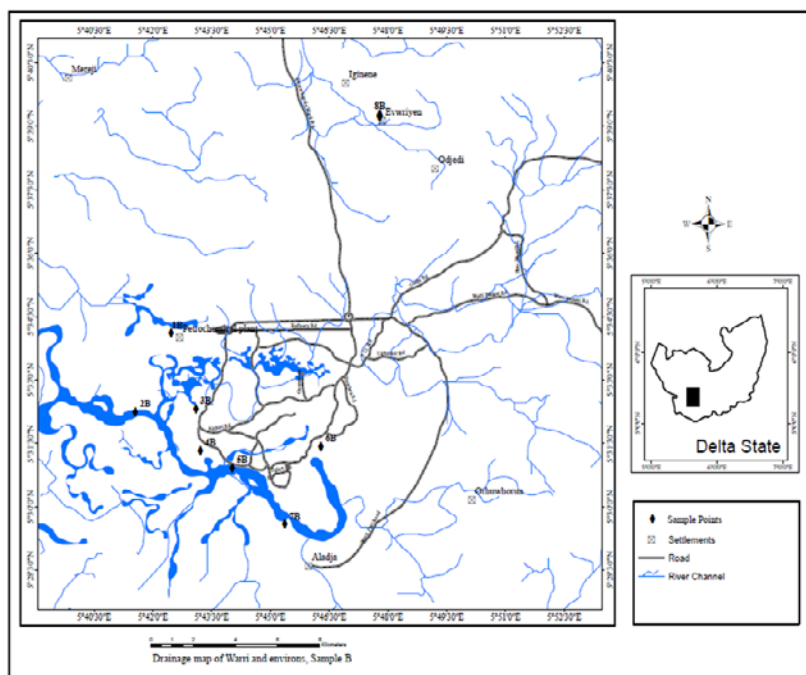


Fig.2. Drainage Map of Warri and Environs and Sample Locations

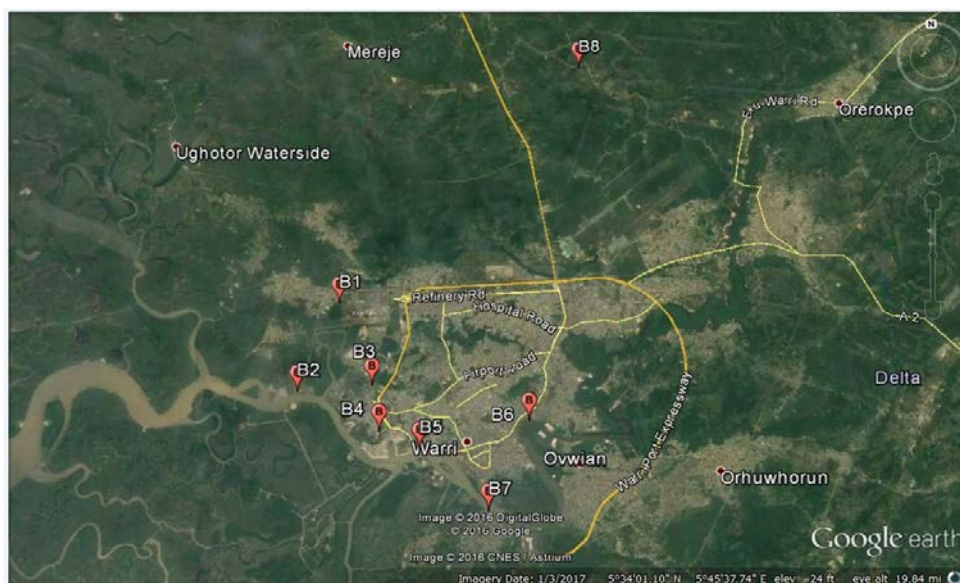


Fig. 3. Aerial Photograph of Warri and Environs showing Sample Locations

5 Sediment Sampling and Chemical Analysis

The stream sediments were collected during the raining and dry season along the Warri river and its tributaries (Fig. 2) and Ewriyen stream (the control) using a hand trowel. The samples were immediately placed into well labeled bags made from soft cloth material.

The samples were pretreated of debris and dried at 105°C in a moisture extraction oven overnight. The dried samples were sieved mechanically using a 0.5mm sieve homogenized and ground to 0.063mm fine powder.

1.0g of each sample was digested using 5ml(3:2) nitric (HNO_3) and perchloric (HClO_4) acid on sand bath evaporated to near dryness. The digested samples were then leached with 5ml of dilute HCl. The residue was washed several times into 100ml volumetric flask and made up to mark. The trace metals in the digest were determined by atomic absorption spectroscopy (Ramirez – Munoz 1968). Accuracy of the analytical method was evaluated by comparing the expected metal concentrations in certified reference materials with the measured values. Simultaneous performance of analytical blanks, standard reference and duplicate samples showed that the accuracy of method was within acceptable limits.

6 Data Analysis

All mathematical and statistical computations were carried out using Microsoft (office) Excel 20B software and SPSS (ver 22).

The multivariate statistical analyses were applied to the data, standardized through Z-scale transformation to avoid misclassification due to wide differences in data dimensionality (Yang et al., 2009). The correlation matrix which was based on calculating the Pearson's correlation coefficient was utilized for displaying relationships between variables. In this way the relationships were easier to interpret since only values between +1 and -1 were taken (Navarro et al, 2008).

Mathematically, principal component analysis (PCA) and Factor Analysis (FA) involve the following five (5) major steps.

(i) Start by coding the variables to have zero means and unit variance.(ii) Calculate the covariance matrix, (iii) find eigenvalues and corresponding eigenvectors, (iv) discard any component that only account for small proportion of variation in data set, (v) develop the factor loading matrix and perform varimax rotation on the factor loading matrix to infer the principal parameters (Lokhande, et al., 2008). In this study, only components or factors exhibiting an eigenvalues of greater than one were retained (Reghunath et al., 2002).

7 Hierarchical Cluster Analysis

Cluster analysis was performed to further classify elements of different sources on the basis of similar chemical properties. In order to discriminate the distinct groups of heavy metals of natural or anthropogenic sources, the result obtained from a hierarchical cluster enabled the identification of elements (Harikumar et al., 2010). Hierarchical cluster analysis was used to find the true groups of data. Cluster analysis was performed on the normalized data sets by means of the Ward's method, using squared Euclidean distances as a measure of similarity (Laluraj, et al, 2005). The spatial variability in the data sets was determined by cluster analysis, using the linkage distance which represented the quotient between the linkage distances for a particular case divided by the maximal linkage distance. The quotient was then multiplied by 100 to standardize the linkage distance represented on the y-axis.

In clustering, the objects were grouped such that similar objects fell into the same class. Hierarchical clustering joined the most similar observations and successively the next most similar observations (Lokhande et al., 2008). The level of similarity at which observations were merged were used to construct dendrogram. In this study, squared Euclidean distance and Ward's were used to construct dendrogram. A short distance shows that the two objects were similar or close together whereas a long distance indicated dissimilarity (Lokhande et al., 2008). Hierarchical cluster analysis using dendrograms identified relatively homogeneous groups of variables with similar properties and combined clusters until only one was left. (Praveena et al., 2007). Each clustered group showed a

specific and similar ecological state of the ecosystem. For clustering analysis, the data were standardized to equalize the influence of parameters.

8 Factor Analysis

The purpose of factor analysis (FA) is the description of the observed variables in complex environmental compartments by finding summarizing factors, which are often causally explainable (Shakeri et al 2009). The extracted factors reflect the main part of information of the data set. The mathematical principles of actor analysis has been described by Reghunath et al (2002).

For factor analysis varimax and Kaiser normalization rotation method was used (Kaiser, 1958) and also used to find association between parameters so that the number of measured variable can be reduced.

9 Assessment of Sediment Contamination

To evaluate the magnitude of contamination (natural and anthropogenic) in the environment, the enrichment factor (EF) as proposed by Simex and Helz (1981) was computed relative to the abundance of species in source materials to that found in an unpolluted area with similar geology.

The following equation was used to calculate the EF values:

$$EF = \left(\frac{C_m}{CF_e} \right)_{\text{sample}} / \left(\frac{C_m}{CF_e} \right)_{\text{control/background value}}, \text{ where } \left(\frac{C_m}{C_r} \right)$$

Sample is the ratio of concentration of heavy metal (C_m) to that of Fe (CF_e) in the stream sediment and $\left(\frac{C_m}{CF_e} \right)_{\text{control / background value}}$ is the reference ratio in the control/background.

Fe was chosen as the element of normalization because natural sources 1.5% vastly dominate its input. It is the most commonly used normalization factor (Loska et al 2003; Seshan et al., 2010). Fe, particularly the redox sensitive iron-hydroxide and oxide under oxidation condition constitutes significant sink of heavy metals in aquatic system. Even a low percentage of $Fe(OH)_3$, in aquatic system, has a controlling influence on heavy metal distribution. Therefore, Fe is taken as a normalization element while determining enrichment factor (Chakravarty and Patgiri, 2009, Harikumar et al, 2010; Fagbote and Olanipekun, 2010).

Five (5) contamination categories were recognized on the basis of the enrichment factors as follows (Sutherland, 2000)

EF < 2 is deficiency to minimal enrichment

EF 2 – 5 is moderate enrichment

EF 5 – 20 is significant enrichment

EF 20 – 40 is very high enrichment

EF > 40 is extremely high enrichment

As the EF values increase, contributions due to anthropogenic origin also increase.

10 Determination of Contamination Factor (CF)

The level of contamination of soil/sediment by a metal is often expressed in terms of a contamination factor calculated as follows:

Contamination factor = metal content in soil, sediment/background value of the metal.

Where $CF < 1$ refers to low contamination

Where $1 \geq CF \geq 3$ means moderate contamination.

Where $3 \geq CF \geq 6$ indicates considerable contamination

Where $CF \geq 6$ indicates very high contamination (Harikumar and Jisha, 2010). The control point values obtained from unpolluted area with similar geology were used for all the indices.

11 Pollution Load Index (PLI)

The extent of pollution by heavy metals has been assessed by employing the method of pollution load index (PLI) developed by Tomilson et al., (1980) and the relationship is shown below.

$$PLI = (CF * CF_2 * * CF_n)^{1/n}$$

Where CF = contamination factor and n = number of metals, (nine in the present study).

PLI provides a simple, comparative means for assessing a site’s quality which is interpreted as follows:

A value of zero indicates perfection, while a value of one(1) indicates only baseline levels of pollutants present and values above one (1) indicate progressive deterioration of the site’s quality (Tomilson et al., 1980; Harikumar and Jisha, 2010 and Al-Qud et al. 2011).

12 Results and Discussion

Table 1: Sediments Heavy Metal Per Location

Loc	pH	Zn mg/kg	Cu mg/kg	Cd mg/kg	Fe mg/kg	Pb mg/kg	Ni mg/kg	Mn mg/kg	Cr mg/kg	V mg/kg	THC mg/kg	TPC mg/kg
B1	5.4	68.65	11.015	9.525	923.45	1.535	6.51	8.93	3.168	0.358	53.52	55.87
B2	5.925	29.84	8.855	7.12	329.92	0.965	7.1	8.95	0.973	0.565	12.90	6.758
B3	5.65	73.64	9.575	9.55	648.68	1.423	3.695	8.65	1.813	0.578	88.94	61.36
B4	5.125	25.66	14.43	8.55	608.69	1.665	5.145	12.2	1.715	0.508	68.46	47.35
B5	5.925	44.53	19.435	4.14	374.59	7.05	4.745	9.1	0.44	0.378	82.28	70.07
B6	5.425	17.74	13.925	15.915	442.90	2.758	4.87	12	1.12	0.793	92.52	77.98
B7	6.075	27.56	19.17	6.37	382.04	4.895	1.665	10.5	0.538	0.503	8.435	4.77
B8	5.725	29.18	15.295	4.285	318.52	1.225	3.095	12.1	0.38	0.42	14.67	4.28
AV	5.656	39.60	13.96	8.182	503.60	2.69	4.60	10.3	1.27	0.51	52.71	41.05

Table 2: Correlation Matrix of Location B1- B8 Sediments Heavy Metals

		pH	OrgC	Zn	Cu	Cd	Fe	Pb
Correlation	pH	1.000	.047	-.477	-.465	-.767	-.762	-.528
	OrgC	.047	1.000	.252	.193	-.067	.089	.225
	Zn	-.477	.252	1.000	.736	.412	.643	.386
	Cu	-.465	.193	.736	1.000	.475	.582	.567
	Cd	-.767	-.067	.412	.475	1.000	.846	.517
	Fe	-.762	.089	.643	.582	.846	1.000	.591
	Pb	-.528	.225	.386	.567	.517	.591	1.000
	Ni	-.387	.337	.666	.601	.326	.384	.372
	Mn	-.414	-.370	-.083	-.066	.580	.501	.058
	Cr	-.496	.229	.494	.303	.325	.490	.176
	V	.083	-.197	-.157	-.104	-.024	-.190	-.329
	THC	-.206	.393	-.033	-.016	.195	.204	.260

		Ni	Mn	Cr	V	THC
Correlation	pH	-.387	-.414	-.496	.083	-.206
	OrgC	.337	-.370	.229	-.197	.393
	Zn	.666	-.083	.494	-.157	-.033
	Cu	.601	-.066	.303	-.104	-.016
	Cd	.326	.580	.325	-.024	.195
	Fe	.384	.501	.490	-.190	.204
	Pb	.372	.058	.176	-.329	.260
	Ni	1.000	-.229	.410	.102	.226
	Mn	-.229	1.000	.025	.071	.148
	Cr	.410	.025	1.000	.118	.218
	V	.102	.071	.118	1.000	.216
	THC	.226	.148	.218	.216	1.000

The correlation matrix in Table 2 revealed significant correlation ($r = >0.70$) between Zn - Cu, Cd-Fe, pH-Cd (neg) and pH-Fe(neg.) which suggests a common origin(Yisa et al., 2011). Some of the sediments heavy metals exhibited poor to mild correlation with all measured parameters and this denote diverse source or origin (Ata et al.2009).

Table 3.Varimax Rotated Factor Analysis of Sediments Heavy Metals

Component	Initial Eigenvalues			Rotation Sums of Squared Loadings		
	Total	% of Variance	Cumulative %	Total	% of Variance	Cumulative %
1	4.777	39.810	39.810	3.357	27.975	27.975
2	2.083	17.360	57.170	3.100	25.831	53.806
3	1.442	12.015	69.185	1.563	13.029	66.835
4	1.213	10.110	79.295	1.495	12.460	79.295
5	.764	6.368	85.662			
6	.485	4.044	89.706			
7	.353	2.945	92.651			
8	.282	2.347	94.999			
9	.212	1.769	96.767			
10	.172	1.434	98.201			
11	.156	1.296	99.497			
12	.060	.503	100.000			

The Factor analysis performed on the sediments heavy metal extracted four factors which accounted for 79.3% of the total variance(Tables 3 and 4).Factor one consists of high factor loading on Zn, Ni, Cu and Cr and reflects anthropogenic input from petroleum related activities (Riccardi et al., 2008). Factor two is dominated by Cd, Mn and Fe with negative loading on pH and suggests anthropogenic input from indiscriminate dumping of metal scraps in streams and effluents from iron/steel foundry industries around the area. Factor three has high loading on THC and OrgC and reflects anthropogenic input from the various hydrocarbon spill in the area. Factor four is dominated by V with negative loading on Pb and suggests anthropogenic input from petroleum refinery and vehicular emission in the study area.

Table 4: Factor Loading of Sediments Heavy Metals

	Component			
	1	2	3	4
Zn	.884	.164	-.050	-.160
Ni	.831	.008	.246	.076
Cu	.803	.212	-.051	-.253
Cr	.595	.247	.242	.282
Cd	.336	.858	.051	-.078
Mn	-.306	.856	-.084	.123
Fe	.497	.776	.103	-.214
pH	-.444	-.755	-.078	.065
THC	-.043	.242	.892	.179
OrgC	.299	-.315	.722	-.288
V	.029	-.003	.073	.908
Pb	.378	.409	.298	-.556

The Q-mode Cluster analysis performed on the sediment heavy metals extracted three major clusters. Cluster one consists of locations 1, 6 and 4 with one and 6 exhibiting great similarity. Cluster two is made up of locations 2 and 7. Cluster three comprises locations 3, 5 and 8 with 3 and 5 displaying some degree of similarity. Cluster one is related to Clusters two and three at maximum distance of 25, while Clusters two and three are related at euclidian distance of 18 (Fig.4.).

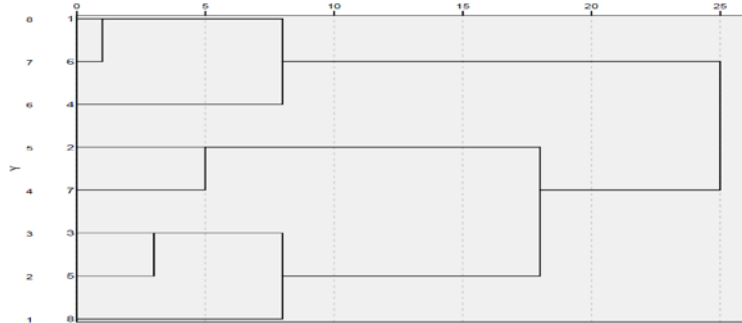


Figure 4. Q-mode Cluster Analysis of Sediments Heavy Metals

The R-mode cluster analysis performed on the sediments heavy metal extracted three clusters (Fig.5). Cluster one consists of Zn, Cu, OrgC, THC, Cd, and Mn. In this cluster, both Cu and Zn, as well as Cd and Mn exhibit great similarity. This cluster is similar to Factors one, two and three to some extent. Cluster two is made up of Cr, V, Pb and Ni and exhibits some similarity with factors one and four. Cluster three on the other hand is made up of pH and Fe and partly similar to factor two.

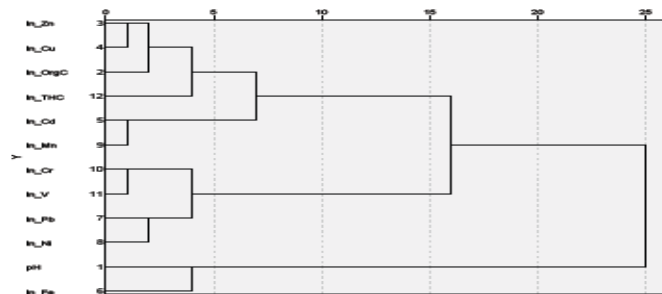


Figure 5: R-mode Cluster Analysis of Sediments Heavy Metals

13 Sediments Contamination Factor

The average contamination factor values for the sediments heavy metals range from 0.686 for Cu to 3.718 for Cr (Table 5).

The ranked order of contamination factor (CF) among the heavy metals was as follows (Table 5): Cr > Mn > Fe > Pb > V > Ni > Cd > Zn > Cu

Cr had a maximum sediments average contamination factor value of 3.72 while a minimum average value of 0.69 was obtained for Cu (Table 5.). Based on Hakanson, 1980 indices, Cr had very high range of contamination at location B1, with considerable contamination level at locations B2, B3, B4 and B6, while locations B5 and B7 recorded moderate range of Cr contamination. Locations B1-B7 were moderately contaminated by Mn, Fe, Ni, Pb, V, Zn and Cd, while low Cu contamination was obtained at several locations (Fig.6).

	Table 5. Sediments Contamination Factor									Pollution Load Index
	Zn	Cu	Cd	Fe	Pb	Ni	Mn	Cr	V	
B1	0.939574	0.369624	1.164486	1.886088	1.372121	1.109459	1.635425	6.964318	0.900806	1.3169191
B2	0.857983	0.487393	0.837674	1.036285	0.741450	2.031887	1.828588	3.534199	1.288936	1.1835053
B3	1.548675	0.392983	1.116519	2.553461	1.150372	1.001923	2.360590	4.229381	1.542518	1.463498
B4	0.988412	0.902535	1.345879	2.149058	2.598611	0.954886	1.649486	4.688781	1.239057	1.5799739
B5	1.294454	0.748779	0.664832	1.492275	1.612216	0.931473	2.839412	1.052348	1.047496	1.1824772
B6	0.521427	0.967798	0.974299	1.258983	1.354750	1.446635	1.869381	3.776467	1.543229	1.3321991
B7	0.849703	0.931623	1.257864	1.214725	1.130584	0.128300	2.378833	1.779327	0.824475	0.9469507
	1.000000	1.000000	1.000000	1.000000	1.000000	1.000000	1.000000	1.000000	1.000000	1
Average	1.000033	0.685819	1.051650	1.655839	1.422872	1.086366	2.080245	3.717832	1.198074	

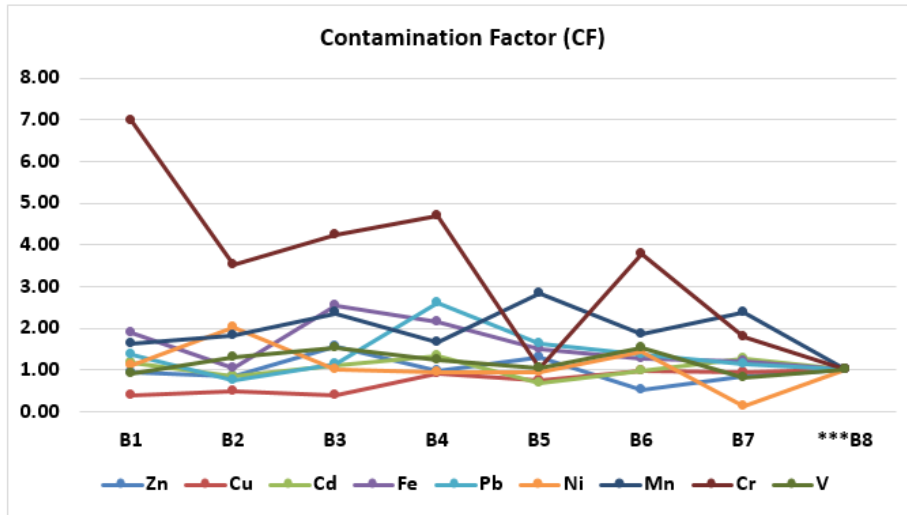


Figure 6: Contamination Factor Graph of Locations B1 – B8 Sediments Sediments Pollution Load Index (PLI)

The pollution load index (PLI) revealed that location B4 had maximum pollution load index of 1.58 and a minimum pollution load index value of 0.95 was obtained at location B7 (Table 5). The order of pollution load index per location for the sediments was as follows:

$$B4 > B3 > B6 > B1 > B2 > B5 > B7.$$

Based on Tomilson et al., 1980 indices, locations B1 to B6 have shown progressive site deterioration with respect to the measured nine (9) heavy metals, while location B7 had only baseline level of pollutants present (Figs.7 and 8).

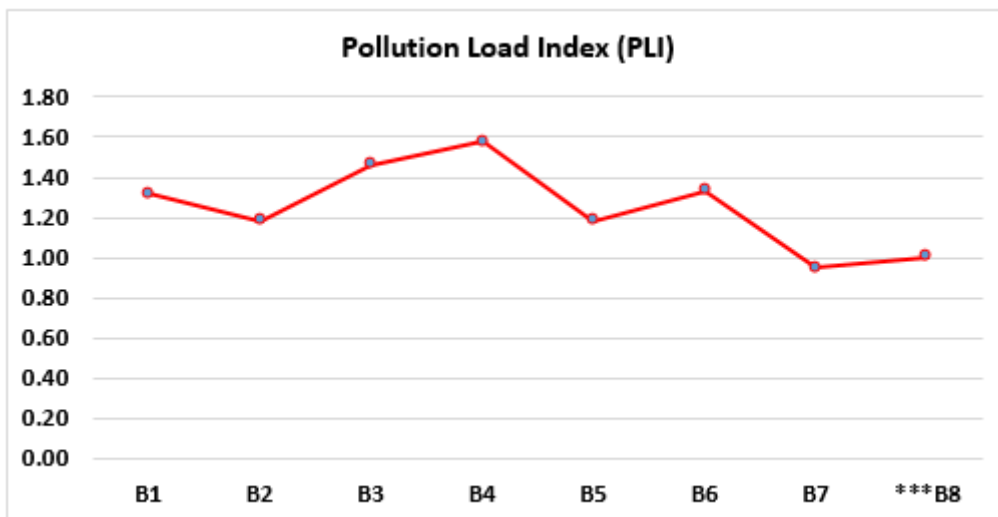


Figure 7: Pollution Load Index (PLI) Graph of Locations B1 – B8 Sediments

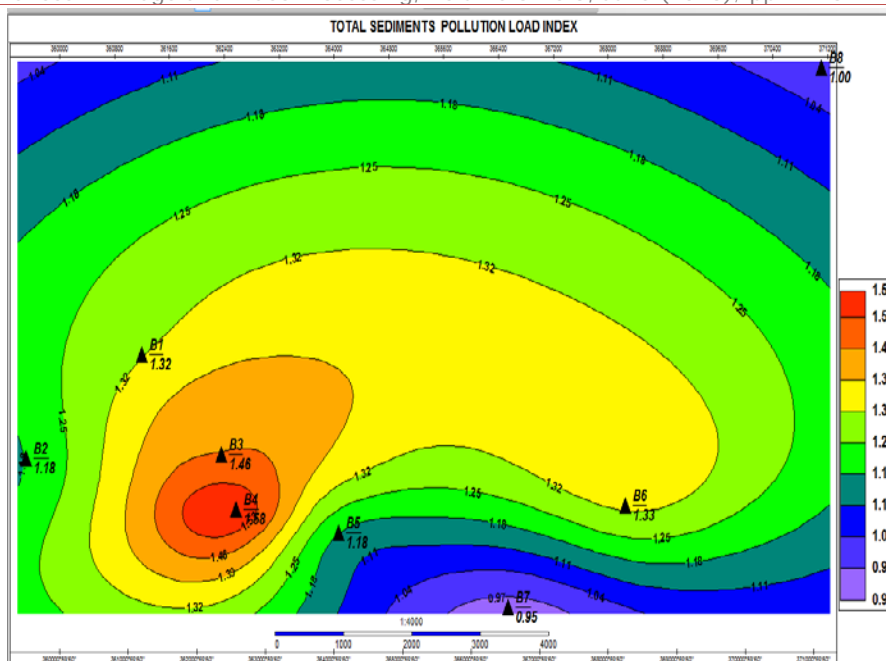


Figure 8: Sediments Pollution Load Index Map of Locations B1-B8.

14 Sediments Enrichment Factor

The enrichment order for the heavy metals of locations B1 – B7 sediments sample was as follows:

Cr > Mn > Fe > Pb > V > Ni > Cd > Zn > Cu (Table 6).

An EF values between 0.5 and 2.0 is regarded as within the natural range while ratio greater than 2.0 indicates some enrichment corresponding to anthropogenic input (Ata et al., 2009; Sekabira et al., 2010).

Based on Sutherland's 2000 indices, the enrichment factor showed that Cr was moderately enriched at locations B1, B2, B4 and B6. The other heavy metals (Fe, Zn, Ni, V, Pb, Cd, Mn and Cu) were either depleted to minimal enrichment or had background concentration at several locations (Fig. 9).

	Zn	Cu	Cd	Fe	Pb	Ni	Mn	Cr	V
B1	0.49816	0.195974	0.617408	1	0.727495	0.588233	0.867099	3.692467	0.477605
B2	0.827941	0.470327	0.808343	1	0.715488	1.960741	1.76456	3.410449	1.243805
B3	0.6065	0.153902	0.437257	1	0.450515	0.392379	0.924467	1.656333	0.604089
B4	0.459928	0.419968	0.626265	1	1.209186	0.444328	0.767539	2.181784	0.576558
B5	0.867437	0.50177	0.445516	1	1.080374	0.624196	1.90274	0.705197	0.701946
B6	0.414165	0.768714	0.773878	1	1.076067	1.149051	1.484834	2.999617	1.225775
B7	0.699502	0.766942	1.035513	1	0.930733	0.105621	1.958332	1.464799	0.678734
B8	1	1	1	1	1	1	1	1	1
Average	0.624805	0.468228	0.67774		0.884265	0.752078	1.381367	2.301521	0.78693

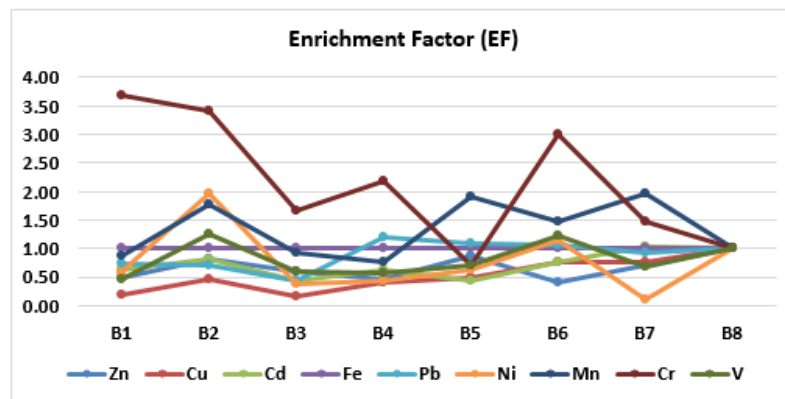


Figure 9: Enrichment Factor(EF) Graph of Locations B1 – B8 Sediments

15 Conclusion

Majority of the heavy metals in the sediments exhibited moderate contamination range at several locations, while Cr has considerably contaminated locations B2, B3, B4 and B6 with high contamination level at location B1.

The computed Pollution Load Index for the sediments heavy metals revealed that locations B1 to B6 have shown progressive site deterioration with respect to the nine (9) measured heavy metals in the area.

The Enrichment Factor for the sediments indicated moderate enrichment for Cr at locations B1, B2, B4 and B6 while Fe, Zn, Ni, V, Pb, Cd, Mn and Cu showed background concentration or were depleted to minimal enrichment at several locations.

REFERENCES

- [1] Abimbola, A. F., Oke, S. A. and Olatunji, A. S., 2002. Environmental Impact assessment of waste dump sites on geochemical quality of water and soils in Warri metropolis, southern Nigeria. *Water Resources*, vol.13, pp.7-11.
- [2] Akpoborie, I. A., Ekakite, O. A. and Adaikpoh, E. O., 2000. The Quality of Groundwater from Dug Wells in Parts of the Western Niger Delta. *Knowledge Review*, vol. 2(5), pp. 72-75.
- [3] Akpokodje, E.G, Etu-Efeotor, J.O., 1987. The Occurrence and Economic Potential of Clean Sand Deposits of the Niger Delta. *J. Afr. Earth Sci.*, vol. 6 (1), pp. 61-65.
- [4] Al-Oud, S.S., Nadeem, M.E.A., and Al-Stibel, B.H., 2011, Distribution of Heavy Metals in Soils and Plants Around a Cement Factory in Riyadh City, Central of Saudi Arabia. *American – Eurasian J. Agric. & Environ. Sci.*, 11 (2): pp. 183 – 191.
- [5] Amajor, L.C., 1991. Aquifers in the Benin Formation (Miocene Recent), Eastern Niger Delta, Nigeria: Lithostratigraphy, Hydraulics, and Water Quality. *Environ Geol Water Sci.*, vol. 17(2), pp. 85-101

- [6] Ata Shakeni; Farid Moore and SoroushModabber, 2009. Heavy metal contamination and distribution in the Shiraz Industrial complex zone soil, south Shiraz, Iran, World Applied Science Journal 6 (3) : 413-425
- [7] Atakpo, E. A. and Akpoboriel.A. 2011. Investigation of sand deposit in parts of Okpe LGA, Delta State, Nigeria. Accepted for Publication: Nig. Jnl. Of Science and Environment.
- [8] Bam T. K. S., 2007. N soil exploration and foundations in the recent coastal areas of Nigeria, Bulletin of Engineering Geology and the Environment, vol. 53, 13-9.
- [9] Benka-Coker, O.M., 1983. Studies of Bacteriological and Physico-chemical parameters of Warri River. M.Sc Thesis, University of Benin.
- [10] Blaser, P., Zimmermann, S. Luster, J. Shotyk, W., 2000. Critical Examination of Trace Element Enrichments and Depletions in Soil: As, Cr, Cu, Ni, Pb and Zn in Swiss Forest Soils. Sc. Total Environ 249 : 257 – 280.
- [11] Chakravarty, M., and Patgiri, A.D., 2009. Metal Pollution Assessment in Sediments of the Dikrong River, N.E. India. J., Hum. Ecol, 27(1); 63 – 67.
- [12] Egborge, A.B.M., 1991. Industrialization and Heavy Metals Pollution in Warri River 32nd Inaugural Lecture, University of Benin, Benin City 1-26
- [13] Egborge, A.B.M., 2001. Water quality index application and industrialization and heavy metal pollution in the warri river, Nigeria.*Environ. Pollut.***12**: 27 – 40.
- [14] Ejechi, B.O., Olobaniyi, S.B., Ogban, F.E., Ugbe, F.C., 2007. Physical and sanitary quality of hand dug well water from oil producing area of Nigeria, Environmental Monitoring and Assessment 128, 495- 501.
- [15] Fagbote E.O. and Olanipekun E.O., 2010. Evaluation of the Status of Heavy Metal Pollution of Sediment of Agbabu Bitumen Deposit area, Nigeria. European Journal of Scientific Research. Vol. 41, Nos. 3, pp. 373 – 382.
- [16] Fagbote, E.O. and Olanipekun, E.O., 2010. Evaluation of the status of heavy metal pollution of soil and plant (*chromolaenaodorata*) of Agbadu Bitumen Deport Area, Nigeria. American-Eurasian J. Sci. Res., 5(4): 241- 248.
- [17] Hakanson, I., 1980. Ecological Risk Index for Aquatic Pollution Control, a Sedimentological Approach. Water Res., 14:975-1001.
- [18] Harikumar, P.S., and Jisha, T.S., 2010. Distribution Pattern of Trace Metal Pollutants in the Sediments of an Urban Wetland in the Southwest Coast of India. International Journal of Engineering science and Technology, Vol. 2(5), pp. 840 – 850.
- [19] Idress, F.A. (2009). Assessment of trace metal distribution and contamination in surface soils of Amman, Jordan. Jour. Chem. 4(1) p77 – 87.
- [20] Imeokparia, E.G.; Onyeobi, T.U.S and Abodunde, F.L., 2009. Heavy metal concentration in soil from a mechanic village in Uvwie Local Government area of Delta State. Nig. Jour, Applied Science Vol. 27 p.144-150.

- [21] Laluraj, C.M., Gopinath, G., Dineshkumar, P.K., 2005: Ground water Chemistry of Shallow aquifers in the Coastal zones of Cochin, India. *Applied Ecology and Environmental Research* 3(1), pp. 133-139.
- [22] Linnik, P.M and Zubenko, I.B. (2000). Role of Bottom Sediments in the Secondary Pollution of Aquatic Environment by heavy metals, Lakes and Reservoirs. *Resource Management* 5(1) pp 11 – 21.
- [23] Lokhande, P.B., Patit, V.V., and Mujawar, H.A., 2008. Multivariate Statistical Analysis of Groundwater in the Vicinity of Mahad Industrial area of Konkan region, India. *International Journal of Applied Environmental Sciences*.
- [24] Loska, K., Wiechula, D. Barska B., Cesule, E., Chojnecka A. (2003). Assessment of arsenic enrichment of cultivated soils in Southern Poland. *Pol. J. Environ. Stud.* 12(2) p 187 – 192.
- [25] Ministry of Commerce and Industry, (2001). *Industrial Mineral Raw Material Resources Survey in Delta State*. MC&I, Asaba. 150p.
- [26] Mohiuddin, K.M; Zakir, H.M, Otomo, K., Sharmin S. and Shikazono, N., (2010) Geochemical Distribution of Trace metals pollutants in water and sediments of downstream of an urban river. *Int. J. Environ. Sci. Tech.* 7(1) p 17-28.
- [27] Navarro, M.C., Pere-Sirvent, C., Martinez – Sanchez., Vidal, J., Tovar, P.J. and Bech, J., 2008. Abandoned mine sites as a source of contamination by heavy metals: A Case study in a semi-arid zone. *Journal of Geochemical Exploration* 96pp 183 – 193.
- [28] Ndiokwere, C.L., 1984. An investigation of the heavy metal content of sediments and algae from the River Niger and Nigerian Atlantic Coastal waters. *Environ. Pollution* 7 (B) 247-254.
- [29] NEDECO, 1954. (Netherlands Engineering Consultant), *The waters of western Nigeria Delta*, The Haque
- [30] Nigerian Meteorological Agency, 2003. *Warri Meteorological Bulletin*. In: *National Meteorological Report*.
- [31] Nigerian Navy, 1982. *Tide Table Containing tidal predictions for Lagos, Escravos bar, Forcados bar, Bonny town and Calabar*, 36pp
- [32] Olabaniyi, S.B., Ogban, F.E. Ejechi, B.O., Ugbe, F.C., 2007a. Quality of Groundwater in Delta State, Nigeria. *Journal of Environmental Hydrology*. 15.
- [33] Praveena, S., M., Ahmed, A., Radojevic, M., Abdullah, M.H. and Aris, A.Z., 2007. Factor –Cluster Analysis and Enrichment Study of Mangrove Sediments - An Example from Mengkabong, Sabah. *The Malaysian Journal of Analytical Sciences*. Vol. 11, no. 2, pp. 421 – 430.
- [34] Ramirez-Munoz, J., 1968. *Atomic Absorption Spectroscopy and Analysis by Atomic Absorption flame Photometry*. Elsevier Publishing Co., NY.
- [35] Reghunath R.T.R., Sreedhara M., Reghavan B.R., 2002. The Utility of Multivariate Statistical Techniques in Hydrogeochemical Studies; example from Karnataka, India. *Water Research* 36, pp. 2437 – 2442.

- [36] Riccardi, C., di Filippo, P., Pomata, D., Incoronato, F., di Basilio, M., Papini, M.P. and Spicaglia, S., 2008. Characterization and distribution of petroleum hydrocarbons and heavy metals in groundwater from three Italian tank farms. *Sci. Total Environ.*, 393: 50-63.
- [37] Ross S.M., 1994. *Toxic metals in soil-plant systems*. Wiley, Chichester, p 469.
- [38] Salomons, W., and Forstner U. (1980). Trace metal analysis of polluted sediments part II evaluation of environmental impact. *Environ. Techn. Letters* 1, p. 506-517.
- [39] Seaward, M.R.D. and Richardson, D.H.S., 1990. Atmospheric sources of metal pollution and effects on vegetation. Pp.75-92,
- [40] Sekabira, K., Oryem, H.O, Basambo, T.A., Mutumba, G., Kakudidi, E., 2010. Assessment of heavy metals pollution in urban streams and its tributaries. *International Journal of Environment, Science and Technology* 7(3), 435-446.
- [41] Seshan, B.R; Natesan, U.; Deepth, K., (2010). Geochemical and Statistical approach for evaluation of heavy metal pollution in Core Sediments in Southeast coast of India. *Int. J. Environ Sci. Tech.* 7(2) p. 291 – 306.
- [42] Simex, S.A, Heiz, G.R, (1981). Regional geochemistry of trace elements in Chesapeake Bay. *Environ. Geology* 3. P 315-323.
- [43] Sutherland, R.A., 2000: Bed sediment-associated trace metals in an urban stream, Oahu, Hawaii, *Environmental Geology* 39:611-37.
- [44] Tomilson, D.C. Wilson, C.J., Harris, C.R., Jeffrey, D.W., 1980. Problem in Assessment of Heavy Metals in Estuaries and the Formation of Pollution Index. *Helgol. Wiss. Meeresunters*, 33(1-4), 566 – 575 (10 pages).
- [45] United Nations Environmental Protection/Global Program of Action (UNEP/GPA), 2004. Why the Marine Environment needs Protection from Heavy Metals. UNEP/GPA Coordination Office. <http://www.oceansatlas.org/unatlas/uneptextph/wastesph/2602gpa>.
- [46] Vermette S.J. and Bingham V.G., 1986. Trace elements in Frobisher Bay rainwater. *Arctic* 39 (2): 177-179
- [47] Vermette S.J. and Bingham V.G., 1986. Trace elements in Frobisher Bay rainwater. *Arctic* 39 (2): 177-179.
- [48] Wanga, M.S; Kanasiime F., Denny P., Scullion J. (2003). Heavy metals in Lake George Uganda with relation to metal concentration in tissues of common fish specie *Hydrobiologia* 499(1-3) pp. 83-93.
- [49] Wigwe, G.A., 1975. The Niger Delta Physical. In Ofomata, G.E.K., (Ed.), *Nigeria in Maps: Eastern States* (pp 38 – 40). Benin: Ethiope Publ. House.
- [50] Yang, Li; Linyu, Xu, Shun, Li 2009. Water quality analysis of the Songhua River Basin using multivariate techniques. *Journal of Water Resources and Protection (JWARP)*
- [51] Yisa, J., Jacob, J.O. and Onoyima, C.C., 2011. Identification of sources of heavy metals pollution in road deposited sediments using multivariate statistical analysis. *J. Emerg. Trends in Eng. Appl. Sci.*, 2: 658-663.

Traffic Sign Detection and Recognition for Driving Assistance System

¹Huei-Yung Lina, ²Chin-Chen Chang, ³Shu-Chun Huang

^{1,3}*Department of Electrical Engineering and Advanced Institute of Manufacturing with High-tech Innovations, National Chung Cheng University, Chiayi 621, Taiwan;*

²*Department of Computer Science and Information Engineering, National United University, Miaoli 360, Taiwan;*

ccchang@nuu.edu.tw

ABSTRACT

In this paper, we present a traffic sign detection and recognition for a driving assistance system. The proposed approach consists of two subsystems for detection and recognition. First, the road sign detection subsystem adopts the color information to filter out most of irrelevant image regions. Image segmentation and hierarchical grouping are then used to select candidate regions of road signs. For the road sign recognition subsystem, a convolutional neural network (CNN) is adopted to classify traffic signs for candidate regions. Experimental results show that our approach can obtain the desired results effectively.

Keywords: Traffic Sign Detection; Traffic Sign Recognition; Color Feature; Neural Network.

1 Introduction

Because of different types of sensing and positioning technologies, driving assistance becomes a popular research topic. For unmanned vehicles and driving assistance systems, the safety problem is always the highest priority compared with the convenience or practicality for a project or system designer.

When driving a vehicle, a driver can get different messages according to local road signs. Traffic signs are often designed with eye-catching colors and easy-to-understand symbols. However, if a driver drives in a complex environment or a driver mental state is not well, this might cause the driver to overlook messages from traffic signs. If there is an automatic detection and recognition system for traffic signs [2, 7, 12, 13, 14, 19], it can report correct traffic signs quickly to the driver and also reduce the burden of the driver. When the driver ignores a traffic sign, the system can give a timely warning. If this system is used in an unmanned vehicle, it can help the automatic driving system to judge the road condition. Hence, the safety of the vehicle driving is greatly improved and the risk of accidents can be reduced.

In this paper, we focus on the detection and identification of traffic signs for driving assistance systems. In addition to testing the system performance, we also experiment with a combination of different system architectures. We first filter out most of the nonsign parts of an image using the color information. Then we extract regions where may have image blocks, and further extract candidate regions from the above image blocks. Finally, we use a convolutional neural network (CNN) to verify the candidate areas of non-road signs and identify the type of the traffic sign.

This paper is structured as follows: Section 2 reviews related works. Section 3 describes our system structure. Section 4 describes the experimental results. Finally, Section 5 presents the conclusions.

2 Related Works

scalera et al. [7] proposed an approach for detecting traffic signs using a hue- saturation-intensity (HSI) color space. They first converted the color space of an image to an HSI color space, and then found the obvious red according to the range of hue and saturation. Similar approaches based on a hue-saturation-value (HSV) color space have also been applied [13, 14, 19]. Shaposhnikov et al. [21] and Vitabile et al. [22] used an HSI color space to define the red area outside the mark and made further retrieval. Miura et al. [18] first converted the color space of an image to a YUV color space, and to select the red and blue range. In terms of geometric and gradient characteristics, Broggi et al. [5] used pre-defined templates to align normalized color modules. If its similarity is greater than a threshold, the shape can be determined.

Escalera et al. [8] used a known angle mask and matched the pre-set search range to detect triangular traffic signs of the three vertices or circular traffic signs on its circumference after capturing a specific color. The slope with the absolute value 1 of the four specific circle points is used then determine the shape and range. Belaroussi and Tarel [3, 4] abandoned the use of color information and focused on the shape features for sign detection. Bahlmann et al. [2] used Haar features to deal with color information. They used AdaBoost and Bayesian classification training to achieve the purpose of road sign detection and identification. Kuo and Lin [16] adopted a Hough transform and corner detection and other methods to detect traffic sign locations, and then used an RBF neural network with a K-d tree to identify traffic signs.

Greenhalgh and Mirmehdi [11] first converted the color space of an image to the HSI color space, and then used maximally stable extremal regions (MSER) to filter circle traffic sign locations. They used the histogram of oriented gradient (HOG) features and the SVM classifier to perform the traffic sign identification. Maldonado-Bascon et al. [17] first screened the images in an RGB color space, selected the red area with an aspect ratio to perform the restriction, and bound selected traffic signs of the candidate area. Then the distance to borders (DtB) features are extracted from the region, and the support vector machine (SVM) classifier was used to train and classify the traffic signs. Fang et al. [9] used a neural network as a basis and the image color and shape as features, and input into the two types of neural networks in order to achieve effect detection. The Kalman filter was then used to predict the possible position of the next frame under the traffic sign. There are several approaches using a deep learning to identify road signs. Some works [6, 20] used a CNN relying on the network to iterate the appropriate weight, and designed the traffic sign identification system.

3 The Proposed Approach

In our system, we first use a color filter and selective search as a detection subsystem. A large number of candidate areas will be detected and then input into the CNN for the final screening and identification.

3.1 Color Information

In our system, we choose HSI as our bases for color judgement. The reason is that this color space only uses one channel to represent the color interval. It has a range of values between 0 and 360 degrees. Because of the above properties, HSI is subject to minimal changes in light and shadow. The process is shown in Fig. 1.

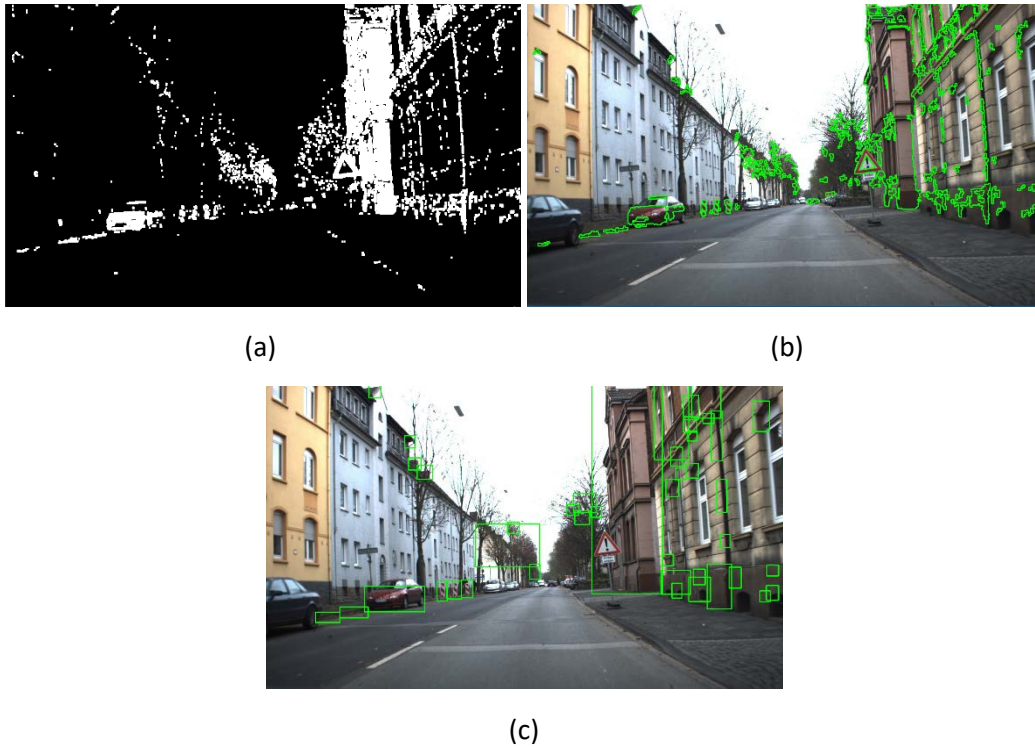


Figure 1. Color selection process. (a) The binary image obtained according to the filter; (b) Select the object outline box based on the binary image; (c) Save a rectangular image according to the object contour

3.2 Selective Search

In general, a way to find objects from an image can be divided into two steps. First, select possible locations from an image. Second, extract features from the candidate area and recognize it. For the first step, we use selective search to identify possible regions. The calculation process of selective search is first to segment an image into a large number of super pixels as initial split areas. Hierarchical grouping is then used to combine the initial division areas. The merged large area is the candidate which will be used for identification in the later stage.

The existing algorithms usually perform the exhausted search, but it can only identify the subjects in the region within its kernel. To prevent the loss of any targets, the exhausted search uses a simple but violent way to solve this problem. It uses a mask to scan the entire area of the image. Because of the uncertainty of the target object size, the exhausted search needs to repeat search for all images with different kernel sizes. The computation complexity of the exhausted search is large. Therefore, its major drawback is the long processing time. The selective search has three advantages. First, the selective search can identify different sizes of objects with the strategies of image segmentation and hierarchical grouping. Second, the basis to distinguish includes color, texture, size and region similarity. Based on the parameters and weights, it can be implemented for most situations. Third, the processing speed is higher compared to the exhausted search. As a result, the selective search is able to produce a lot of candidate regions with high speed. The process is shown in Fig. 2.

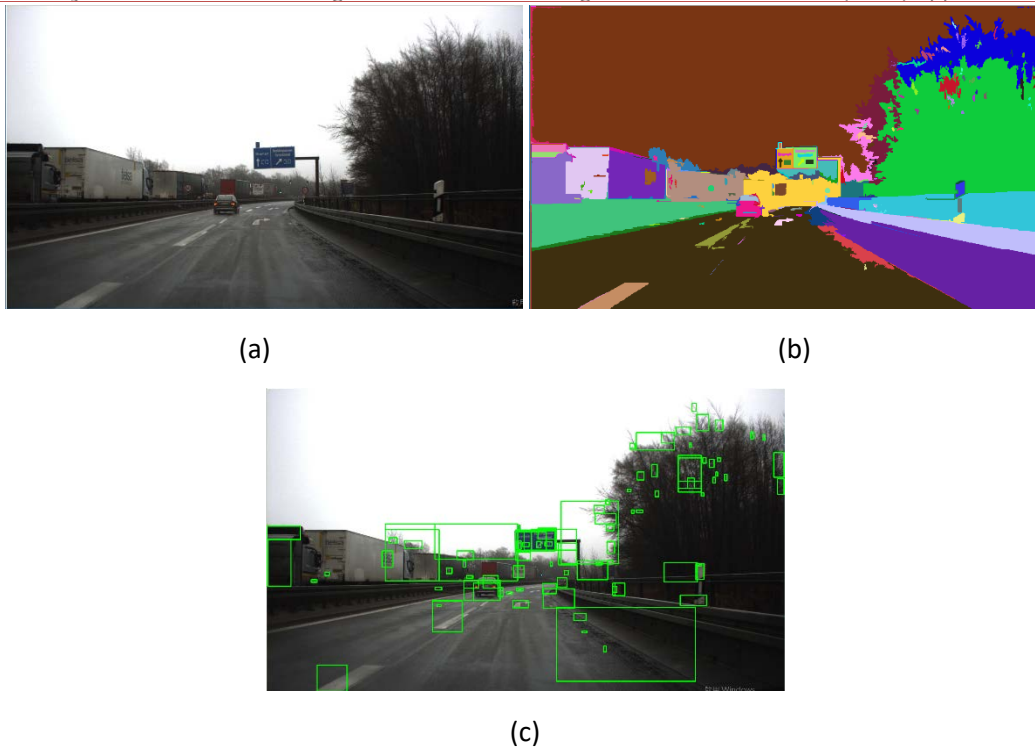


Figure 2. The process diagram of the selective search. (a) The source image; (b) Image segmentation; (c) The results of the selective search

In addition, because the target objects have different characteristics, according to different situations, the selective search has some strategies to implement. Here, three different strategies are listed as follows: 1) Since the selective search algorithm requires hierarchical merging for the initial regions, it is important to use different initial algorithms according to the situations. 2) Use different color spaces to extract different color attributes. 3) In the case of region consolidation, we can change the estimation of region similarity with different situations.

This paper adopts a graph-based image segmentation approach [10]. The algorithm uses image pixel as unit, according to the dissimilarity between the pixels, to determine whether two pixels are in the same region. The pixels are compared to the surrounding area in eight directions, and the similarity in eight directions is arranged from small to large, e_1, e_2, \dots, e_N . The computation for its dissimilarity is as follows:

$$\sqrt{(r_1 - r_2)^2 + (g_1 - g_2)^2 + (b_1 - b_2)^2},$$

where r_i, g_i , and b_i are the three channels of a color space. When the pixels make up a small area, repeat the calculation of dissimilarity so that we can spread to the entire image. In some different circumstances of the local area, the image-based segmentation does not use global thresholds, but adaptive thresholds. The adaptive thresholds are calculated by the interclass between different regions and intraclass in the same region.

About the regional consolidation, the region similarity can be calculated by the image features. We divide the feature similarity into color similarity, texture similarity, size similarity and filling similarity. The color similarity is calculated using three color channels such as hue, saturation and brightness. The texture similarity uses Gaussian function to calculate the differentiation in each direction of all channels. In the end, we can get a texture histogram. The size similarity is based on the number of

pixels in two regions. This is to increase the combined rate of small areas. The texture similarity identifies the border around the region. If the border size of two regions is similar and the overlap area is large, then we merge these two regions. Using the four different similarities above, we can adjust individually according to the real situations. The selective search can produce a large number of candidate regions in a short time, but its disadvantage is also obvious. It has too many post-selected areas in the complex image, which decreases the speed of deep learning. In our system, we have already filtered out most regions with an HSI color space. Therefore, the influence of having too many candidate regions from the selective search can be reduced.

3.3 Convolutional Neural Network

We utilize two kinds of deep learning structures to train our system. One of the structures is Alexnet [15], in which the architecture mainly contains eight layers. The first five layers are convolutional layers and the latter three are all connected layers. In the last layer, we set a 43-way softmax layer to connect with the full connected layer. AlexNet can be considered as an example architecture of a deep convolutional network. There are many network architectures such as ZF-net, SPP-net, VGG and other networks, taking AlexNet as a prototype. AlexNet's success consists of several parts: Rectified Linear Unit (ReLU), pooling, local response normalization and dropout. It not only improves the training speed and accuracy, but also reduces the over-fitting problem.

The second deep learning architecture is GoogLeNet. In the case with a large amount of data, the easiest way to improve the performance of the network is to increase the depth and width of the network. However, it has two problems: 1) A large network generally needs more parameters, and using the fixed data, it is likely to cause the network over-fitting. 2) A large network needs more computing resources. For instance, increasing the number of convolution of the network will lead to increase the computing volume. In addition, if the increase of the network has not been effectively used such as the weight close to zero, it will cause a waste of computing resources. To solve these problems, Arora [1] proposed the construction of inception. The main idea of inception is to find and describe the dense components of the local sparse structure in the convolutional network. It is assumed that translation invariance is established by convolutional blocks and the repetition is spatially extended. We need to find the ideal local structure and expand the duplication in the space. GoogLeNet is also based on the above inception design concept.

4 Results

The experiments are divided into two parts, which are individually tested according to the detection and identification in the system. The datasets are used separately for detection and recognition. We use German Traffic Sign Detection Benchmark (GTSDB) as a dataset for detection and German Traffic Sign Recognition Benchmark (GTSRB) as a dataset for recognition.

For the detection part, we use 300 discrete images in GTSDB dataset for testing. In addition, because the system is designed for red traffic signs, we only record red signs as our ground truth. The correctness of the test is based on whether the candidate area is selected by the selective search and can be correctly extracted with a bounding box. There are two points to check with the benchmark. First, the target area has to be selected more than 80%. Second, the area of the bounding box containing the target should not exceed 1.5 times of the target area. If one of the conditions fails, then we consider the detection incorrect. According to the previous part of the selective search, the algorithm can use different color spaces as its strategy in different situations. Therefore, this experiment in addition to record the accuracy of the detection system, we also test the image segmentation for the selective search in different color spaces for the correction rate.

Table 1 shows the evaluation results. The detection system only focuses on the correct capture of the traffic sign location. The selected region of a road sign is integrated into the identification system. Thus, only the values of true positive, false negative and accuracy are reported in the table. According to the experimental results in Table 1, although the HSI color space is used to reduce the impact of light and shadow changes in the image, it still cannot fully reduce its influence. The reflective light and back-light will cause the detection failure. In different color spaces, although the CIE XYZ gives the highest correction rate, it still cannot distinguish the background from the traffic sign due to their similarity.

Table 1 Selective search in the color space with the accuracy and recall rates, and the red filter screening results

	True positive	False negative	Precision
RGB	238	19	92.6%
HSI	215	42	83.6%
YCrCb	230	27	89.4%
CIE XYZ	241	16	93.7%
CIE Lab	230	27	89.4%
CIE Luv	224	33	87.1%
Red filter	246	11	95.7%

For the recognition part, the part of deep learning is based on Caffe. We have 39209 training images from GTSRB as our training data, which can be divided into 43 road sign categories. The test data are randomly selected 1000 images from GTSRB. The results of training and testing via GoogLeNet are shown in Fig. 3. We use a gradient descent method for the training. The parameters include the basic learning rate set as 0.01, the number of iterations as 100000 times, and the weight attenuation as 0.0002. Fig. 4 shows the results of using AlexNet. The base learning rate is set as 0.01, the number of iterations is 600, and the weight attenuation is 0.0005. With the above parameters, when the iteration is more than 600 times, the model will incur the over-fitting issue.

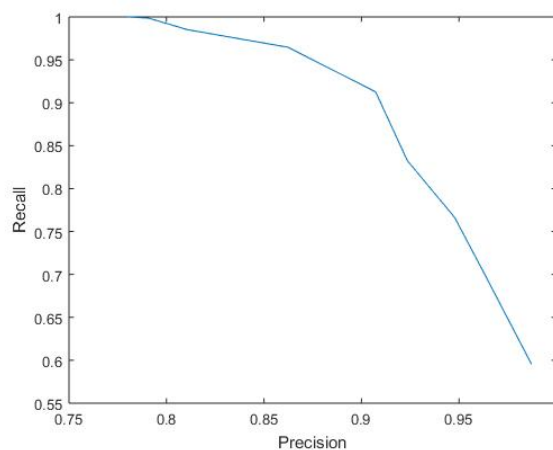


Figure 3. Test result of GoogLeNet

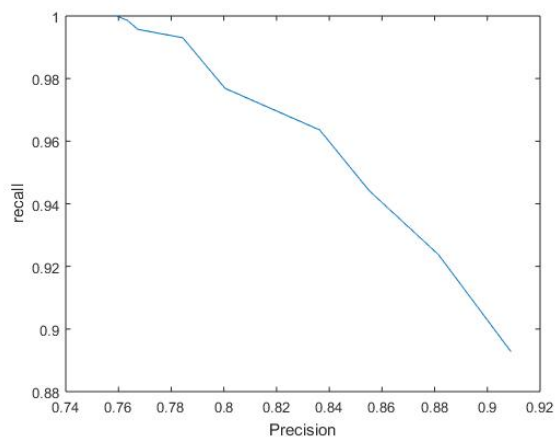


Figure 4. Test result of AlexNet

5 Conclusion

We have presented traffic sign techniques for driving assistance systems. The system can be divided into road sign detection and identification subsystems. The road sign detection system uses the color, the image segmentation and the hierarchical grouping methods to select candidate areas of the road sign. The candidate area from detection is used for identification. We then use a CNN for the road sign recognition system. Results show that the proposed algorithm can obtain the desired results effectively.

ACKNOWLEDGEMENTS

The support of this work in part by the Ministry of Science and Technology of Taiwan under Grant MOST 104-2221-E-194-058-MY2 is gratefully acknowledged.

REFERENCES

- [1] S. Arora, A. Bhaskara, R. Ge, and T. Ma, "Provable bounds for learning some deep representations," in Proceedings of the 31st International Conference on International Conference on Machine Learning - Volume 32, ser. ICML'14. JMLR.org, 2014, pp. I-584-I-592.
- [2] C. Bahlmann, Y. Zhu, V. Ramesh, M. Pellkofer, and T. Koehler, "A system for traffic sign detection, tracking, and recognition using color, shape, and motion information," in IEEE Proceedings. Intelligent Vehicles Symposium, 2005., June 2005, pp. 255-260.
- [3] R. Belaroussi and J.P. Tarel, "A real-time road sign detection using bilateral chinese transform," in Proceedings of the 5th International Symposium on Advances in Visual Computing: Part II, ser. ISVC '09. Berlin, Heidelberg: Springer-Verlag, 2009, pp. 1161-1170
- [4] R. Belaroussi and J.P. Tarel, "Angle vertex and bisector geometric model for triangular road sign detection," in 2009 Workshop on Applications of Computer Vision (WACV), Dec 2009, pp. 1-7.
- [5] Broggi, P. Cerri, P. Medici, P.P. Porta, and G. Ghisio, "Real time road signs recognition," in 2007 IEEE Intelligent Vehicles Symposium, June 2007, pp. 981-986.

- [6] D. Cirean, U. Meier, J. Masci, and J. Schmidhuber, "A committee of neural networks for traffic sign classification," in The 2011 International Joint Conference on Neural Networks, July 2011, pp. 1918–1921.
- [7] De La Escalera, J.M. Armingol, J.M. Pastor, and F.J. Rodriguez, "Visual sign information extraction and identification by deformable models for intelligent vehicles," *Trans. Intell. Transport. Sys.*, vol. 5, no. 2, pp. 57–68, Jun. 2004.
- [8] de la Escalera, L.E. Moreno, M.A. Salichs, and J.M. Armingol, "Road traffic sign detection and classification," *IEEE Transactions on Industrial Electronics*, vol. 44, no. 6, pp. 848–859, Dec 1997.
- [9] C.Y. Fang, S.W. Chen, and C.S. Fuh, "Road-sign detection and tracking," *IEEE Transactions on Vehicular Technology*, vol. 52, no. 5, pp. 1329–1341, Sept 2003.
- [10] P.F. Felzenszwalb and D.P. Huttenlocher, "Efficient graph-based image segmentation," *Int. J. Comput. Vision*, vol. 59, no. 2, pp. 167–181, Sep. 2004.
- [11] J. Greenhalgh and M. Mirmehdi, "Real-time detection and recognition of road traffic signs," *IEEE Transactions on Intelligent Transportation Systems*, vol. 13, no. 4, pp. 1498–1506, Dec 2012.
- [12] S.C. Huang, H.Y. Lin, C.C. Chang. An in-car camera system for traffic sign. Proceedings of the Joint 17th World Congress of International Fuzzy Systems Association and 9th International Conference on Soft Computing and Intelligent Systems, Detection and Recognition, Otsu, Japan, June 2017.
- [13] W.C. Huang and C.H. Wu, "Adaptive color image processing and recognition for varying backgrounds and illumination conditions," *IEEE Transactions on Industrial Electronics*, vol. 45, no. 2, pp. 351–357, Apr 1998.
- [14] D.L. Kellmeyer and H.T. Zwahlen, "Detection of highway warning signs in natural video images using color image processing and neural networks," in *Neural Networks, 1994. IEEE World Congress on Computational Intelligence., 1994 IEEE International Conference on*, vol. 7, Jun 1994, pp. 4226–4231.
- [15] Krizhevsky, I. Sutskever, and G.E. Hinton, "Imagenet classification with deep convolutional neural networks," in *Proceedings of the 25th International Conference on Neural Information Processing Systems*, ser. NIPS'12. USA: Curran Associates Inc., 2012, pp. 1097–1105.
- [16] W.J. Kuo and C.C. Lin, "Two-stage road sign detection and recognition," in *2007 IEEE International Conference on Multimedia and Expo*, July 2007, pp. 1427–1430.
- [17] S. Maldonado-Bascon, S. Lafuente-Arroyo, P. Gil-Jimenez, H. Gomez-Moreno, and F. Lopez-Ferreras, "Road-sign detection and recognition based on support vector machines," *IEEE Transactions on Intelligent Transportation Systems*, vol. 8, no. 2, pp. 264–278, June 2007.
- [18] J. Miura, T. Kanda, and Y. Shirai, "An active vision system for realtime traffic sign recognition," in *ITSC2000. 2000 IEEE Intelligent Transportation Systems. Proceedings (Cat. No.00TH8493)*, 2000, pp. 52–57.
- [19] L. Pacheco, J. Batlle, and X. Cufi, "A new approach to real time traffic sign recognition based on colour information," in *Intelligent Vehicles'94 Symposium, Proceedings of the*, Oct 1994, pp. 339–344.
- [20] P. Sermanet and Y. LeCun, "Traffic sign recognition with multi-scale convolutional networks," in *The 2011 International Joint Conference on Neural Networks*, July 2011, pp. 2809–2813.

- [21] W.D. Shaposhnikov, D.G. Shaposhnikov, L. N, E.V. Golovan, and A. Shevtsova, "Road sign recognition by single positioning of space-variant sensor," in Proc. 15th International Conference on Vision Interface, 2002, p. 2002.

- [22] S. Vitabile, A. Gentile, and F. Sorbello, "A neural network based automatic road signs recognizer," in Neural Networks, 2002. IJCNN '02. Proceedings of the 2002 International Joint Conference on, vol. 3, 2002, pp. 2315–2320.

A Logic Circuit Simulation for Finding Identical or Redundant Files using Counter and Register

¹Lianly Rompis

¹*Electrical Engineering Study Program, Faculty of Engineering,
Universitas Katolik De La Salle Manado;
lrompis@unikadelasalle.ac.id*

ABSTRACT

Computers and internet have become globally used nowadays and also part of the important facilities that could support information exchanges and cloud computing. People deals with texts, images, and videos processing, reaches out the specific goal of their works. It happens that due to much information and procedures, people will have many redundant files such as images or videos in their host computers or terminals, or maybe for some specific reasons people need to find data from big servers that surely have many files with same type and property because people accidentally put them there without knowing others also probably put the same ones. Using the basic concept of sequential logic circuit and electronic workbench 5.12 software, a logic circuit simulation consists of counter and register could be designed to show logically how to a computer or digital machine would interact to find redundant files, images or videos, or same files from many identical data from a server. The methods being used are study literature, analysis, design, and simulation. The output shows an expected result, a logic circuit simulation that could be applied on digital devices for finding identical or redundant files, or other related important process.

Keywords: Redundant Files, Identical Data, Redundant Data, Image and Video, Cloud Computing

1 Introduction

Big Data and Cloud Computing are the essential things recently related to Digital and Information Technologies. Everything is putted in the internet and data is the core of all the information people dealing with. However, have we ever imagined before how many data are being stored and how many data could possibly have the same size, properties, and type because it is being stored many times with different names by someone or being passed among people around the world? This probably will not become a great problem for big data and cloud computing in the future because of the unlimited capacity, but if we can manage those data or files, at least could support efficiency for data storage and server endurance. Using the basic concept of sequential circuit and Electronic Workbench 5.12 software utility, we can build and simulate a logic circuit consists of two main components, counter and register, which can be used to find identical or redundant data such as same images or same videos. It will then would be further sorted for re-selection or automatically deleted.

2 Methods

Learning from several methodologies from [7,8], the methodology being used for this research mainly to understand the basic concept of sequential logic circuit and combine the functions of counter and register, to derive a logic circuit simulation for finding redundant or identical images or videos.

3 Basic Theories

3.1 Asynchronous Counter

Asynchronous Counter is a type of sequential logic circuit functions for counting binary information, which all the input of all the flip-flop components are connected together to logic 1 (standard high dc voltage). The first clock is connected to a clock source, while the other clocks need to be connected to output Q from previous flip-flop, as shown in Figure 1 [1,2,3,4,5,6]. The number of bit depends on number of flip-flop being used. For example, in Figure 1, to have a design output values in 4-bit length, the number of flip-flop that we used is 4 (four) also. The bit-sequences are given in Figure 2 [6].

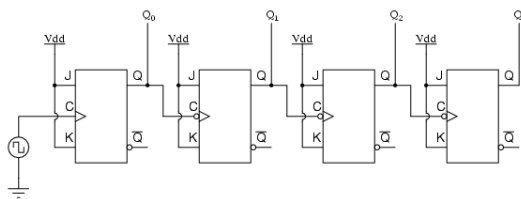


Figure 1. A four-bit asynchronous up counter

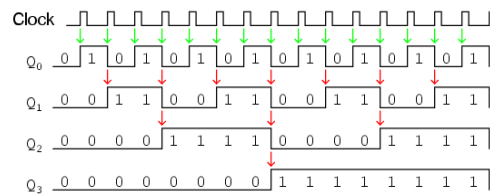


Figure 2. A four-bit asynchronous output waveform ($Q_3Q_2Q_1Q_0$)

3.2 Shift Register

Shift register is another type of sequential logic circuit, mainly for storing digital data. They are a group of flip-flops, usually D-FF, connected in a loop so that the output from one flip-flop becomes the input of the next flip-flop, and so on [1,2,5]. All the flip-flops are driven by a common clock, and all are set or reset simultaneously. This is shown in Figure 3.

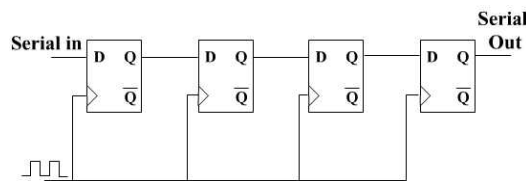


Figure 3. Right shift register

3.3 RS-Flip Flop

Flip-Flop is a basic component of combinational logic circuit and sequential logic circuit, mostly used in building counter and register circuits. The design for flip-flop comes from logic gate circuits. RS-Flip Flop is one of the main flip-flops that normally functions as a latch. It has an input of 2 lines and output of 2 lines as being referred in [1,2,3,4,5].

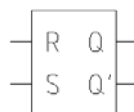


Figure 4. Schematic symbol of RS-FF

A schematic of RS-FF (Reset-Set Flip-Flop) is shown in Figure 4. The state table as the characteristic of it is given in Table 1. The output will not change if the inputs are zeros. If the Reset Input is set to logic 1, the output will be zero, and the reverse, if the Set Input is set to logic 1, the output will be one.

Table 1. Tuth table of an RS flip-flop

INPUTS		OUTPUTS	
R	S	Q _{n+1}	$\overline{Q_n + 1}$
0	0	Q _n	$\overline{Q_n}$
0	1	0	1
1	0	1	0
1	1	-	-

3.4 XNOR Logic Gate

Logic Gates are the basic components of digital logic circuit and the core parts of building a digital computer. One of the important logic gates is an XNOR logic gate. The output of this logic gate is 1 only if the number of logic 1 in inputs is even, as given in Table 2. The schematic symbol is shown in Figure 5 [1,2,3,4,5].



Figure 5. Schematic symbol of 2-input XNOR logic gate

Table 2. Tuth table of a 2-input XNOR logic gate

INPUTS		OUTPUT
0	0	1
0	1	0
1	0	0
1	1	1

4 Analysis and Design

4.1 Analysis

Asynchronous counter functions as a counting circuit, starting from number 0 to number 15. Let's assume the numbers referred as a unique number of files being stored. The files can be called and compared to a file being given as an input to the computer or digital device. In here, we use a 3-bit asynchronous up-counter for simple logic simulation, which ranges from 0 to 7 as shown in Figure 6. This counter is used to call an image or video file according to their unique number, respectively.

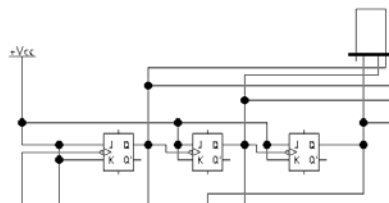


Figure 6. Asynchronous counter for basic simulation

All the files being called will then be compared one by one with the source file being input to the system or computer. Whenever the two compared files are match, the system will send the output and display it. So it will need a comparator for the task. For this logic simulation we can use XNOR gates because of its 'comparing' characteristic, given by Figure 7.

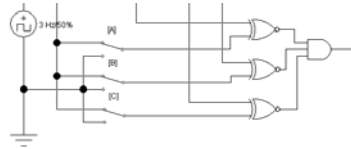


Figure 7. Logical inputs with comparator

The counter will keep count in a loop except we have a controller circuit to arrange the way it counts. That is why we need to add register to store and keep the file and display it on the output. Here we use D-FFs like the following one described in Figure 8.

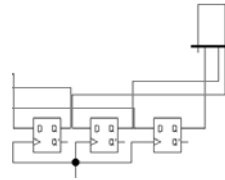


Figure 8. Shift register

4.2 Design

A computer has groups of counter and register that usually built for processing digital information in bits or bytes. All information is stored in registers with a unique number.

This logic circuit connection represents a simple way how actually data can be handled by a logical component known as counter and register. Their logical characteristics might be used as a basic concept for data processing and analysis, especially in organizing data. Figure 9 explains the part of computer architecture and Figure 10 gives the block diagram of further logic simulation that could be done.

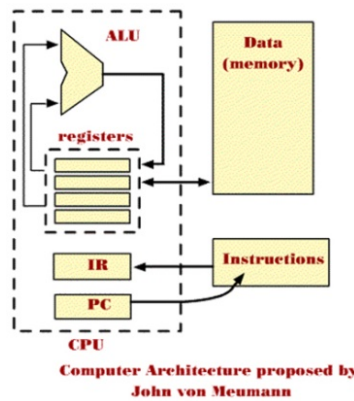


Figure 9. Computer architecture

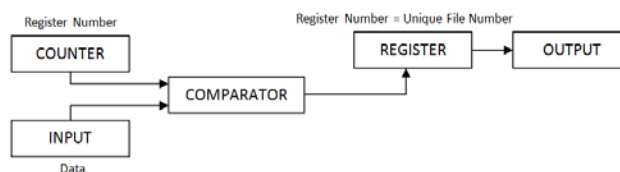


Figure 10. Block diagram for finding file

Based on the given analysis and each component characteristic, in this research counter, register, inputs, and comparator are connected together, as shown in Figure 11.

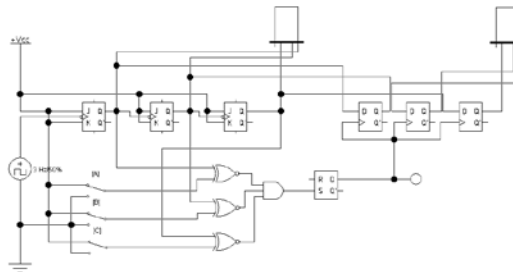


Figure 11. Basic logic circuit simulation with register and counter

The logical inputs will be compared with counting number, and if they have same unique logical number, the file being stored in register would be called and displayed. We can set up and do programming that would stop the counter or make it keeps counting and looking up for other same files.

5 Simulation

From the simulations using software Electronic Workbench 5.12, the designed logic circuit gives the expected outputs. In Figure 12, counter keeps count although same file already displayed.

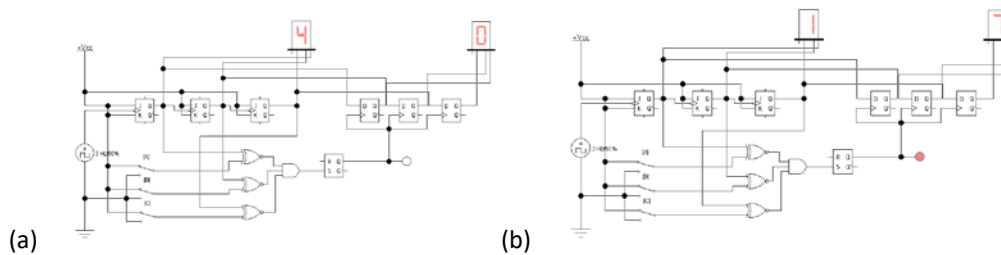


Figure 12. Simulation shows that same file will be displayed but counter keeps counting

Modifying the hardware circuit or program, we can stop the counter as shown in the following Figure 11. After the system detects the same file, counter will stop and register will show the right file on display. It can be started again and do comparison on the same file based on the inputs.

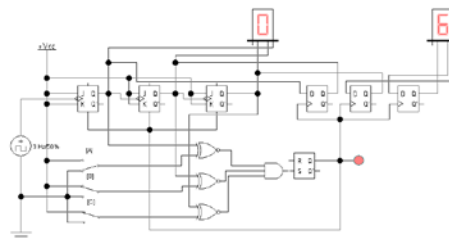


Figure 13. Simulation shows that counter will stop when system detects same file

Again modifying the hardware circuit or program, it happen that we can let the counter keeps counting and register will match and keep changing its file with the counter, as shown in Figure 12.

This is a kind like scan files based on the source file and probably can be used to detect redundant files.

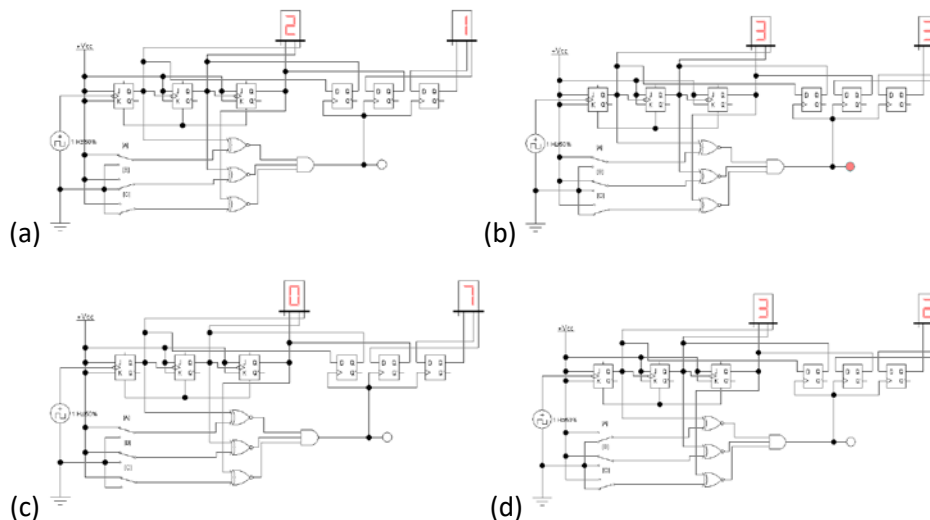


Figure 14. Simulation shows that register will do the comparison every time and display the same file

6 Conclusion

Using Counter and Register, we can build a logic circuit simulation for finding or detecting image or video files for data processing or data efficiency. This is only a basic concept and simple simulation that figures out more clearly about the functions of a counter and a register. The logic circuit simulation assumes that every file could be uniquely characterized in unique logical number (bits or bytes). Same file refers to a file that has a same size, type, properties, and content, although different in name. It can be used for further research development in hardware or software engineering to handle information more efficiently and help user to organize their files and data storage, by finding the same files or removing redundant files in case it is very important to have only one specific and unique file.

REFERENCES

- [1]. Malvino, A., *Elektronika Komputer Digital*. Jakarta: Penerbit Erlangga, 1988.
- [2]. Cavanagh, *Digital Computer Arithmetic Design and Implementation*. McGraw Hill, 1985.
- [3]. Holdsworth, *Digital Logic Design*. Bosterworth, 1982.
- [4]. Tokheim, R., *Prinsip-Prinsip Digital*. Jakarta: Penerbit Erlangga, 1996.
- [5]. Budiharto, W., *Elektronika Digital dan Mikroprosesor*. Yogyakarta: Penerbit ANDI, 2005.
- [6]. All About Circuits, "Asynchronous Counters", All About Circuits.com, 2012.
Source: <https://www.allaboutcircuits.com/textbook/digital/chpt-11/asynchronous-counters/>
- [7]. Sangadji, E. and Sopiah, *Metodologi Penelitian: Pendekatan Praktis dalam Penelitian*. Yogyakarta: Penerbit ANDI, 2010.
- [8]. Semiawan, C.R. and Raco, J.R., *Metode Penelitian Kualitatif: Jenis, Karakteristik, dan Keunggulannya*. Jakarta: Penerbit Grasindo, 2010.